Research Article

Mengxin Wang#, Shuyuan Guo#, Bingling Lin, Tao Lv, Zhuxia Zhang, Die Hu, Azhen Hu, Bingxuan Xu, Yulong Qi, Li Liu#, Guanxun Cheng#, Yun Chen#, Tingting Zheng*#

Ultrasonic-induced reversible blood–brain barrier opening: Safety evaluation into the cellular level

https://doi.org/10.1515/chem-2022-0173
received February 28, 2022; accepted May 27, 2022

Abstract: An important function of the blood–brain barrier (BBB) is to protect the central nervous system and maintain its homeostasis, but it is also a major barrier to the intervention and treatment of neurological diseases. Our study aimed at opening the BBB using a noninvasive method, focused ultrasound, screening for 16 different parameter combinations of frequency, peak voltage (Ppeak) and irradiation time. Comparing the results of hematoxylin–eosin staining, serum oxidative damage factor and TUNEL staining under various conditions, we obtained a parameter combination that did not lead to oxidative stress injury and apoptosis: 0.8 mHz + 900 mVpp + 90 s. It will be used as a safety parameter for BBB opening treatment of Parkinson's disease in our subsequent experiments. In addition, the closing time after the BBB opening was verified in magnetic resonance imaging contrast examination and at the tissue level. It is worth mentioning that, different from previous

*** Corresponding author: Tingting Zheng,** Shenzhen Key Laboratory for Drug Addiction and Medication Safety, Peking University Shenzhen Hospital, Shenzhen Peking University-Hong Kong University of Science and Technology Medical Center, Shenzhen 518036, China, e-mail: kyzs_018@126.com
Mengxin Wang: Shenzhen Key Laboratory for Drug Addiction and Medication Safety, Peking University Shenzhen Hospital, Shenzhen Peking University-Hong Kong University of Science and Technology Medical Center, Shenzhen 518036, China, e-mail: wangmengxin97@163.com
Shuyuan Guo: Shenzhen Key Laboratory for Drug Addiction and Medication Safety, Peking University Shenzhen Hospital, Shenzhen Peking University-Hong Kong University of Science and Technology Medical Center, Shenzhen 518036, China, e-mail: 1010541701@qq.com
Bingling Lin: Department of Imaging, Peking University Shenzhen Hospital, Shenzhen Peking University-Hong Kong University of Science and Technology Medical Center, Shenzhen 518036, China, e-mail: linbling@mail2.sysu.edu.cn
Tao Lv: Shenzhen Key Laboratory for Drug Addiction and Medication Safety, Peking University Shenzhen Hospital, Shenzhen Peking University-Hong Kong University of Science and Technology Medical Center, Shenzhen 518036, China, e-mail: 761285576@qq.com
Zhuxia Zhang: Shenzhen Key Laboratory for Drug Addiction and Medication Safety, Peking University Shenzhen Hospital, Shenzhen Peking University-Hong Kong University of Science and Technology Medical Center, Shenzhen 518036, China, e-mail: 836796250@qq.com
Die Hu: Shenzhen Key Laboratory for Drug Addiction and Medication Safety, Peking University Shenzhen Hospital, Shenzhen Peking University-Hong Kong University of Science and Technology Medical Center, Shenzhen 518036, China, e-mail: 2470464131@qq.com
Azhen Hu: Shenzhen Key Laboratory for Drug Addiction and Medication Safety, Peking University Shenzhen Hospital, Shenzhen Peking University-Hong Kong University of Science and Technology Medical Center, Shenzhen 518036, China, e-mail: H20130727@126.com

# Equal contribution.

Bingxuan Xu: Shenzhen Key Laboratory for Drug Addiction and Medication Safety, Peking University Shenzhen Hospital, Shenzhen Peking University-Hong Kong University of Science and Technology Medical Center, Shenzhen 518036, China, e-mail: 924375303@qq.com
Yulong Qi: Department of Imaging, Peking University Shenzhen Hospital, Shenzhen Peking University-Hong Kong University of Science and Technology Medical Center, Shenzhen 518036, China, e-mail: 570020720@qq.com
Li Liu: Shenzhen Key Laboratory for Drug Addiction and Medication Safety, Peking University Shenzhen Hospital, Shenzhen Peking University-Hong Kong University of Science and Technology Medical Center, Shenzhen 518036, China, e-mail: liuli126126@126.com
Guanxun Cheng: Department of Imaging, Peking University Shenzhen Hospital, Shenzhen Peking University-Hong Kong University of Science and Technology Medical Center, Shenzhen 518036, China, e-mail: 18903015678@189.cn
Yun Chen: Shenzhen Key Laboratory for Drug Addiction and Medication Safety, Peking University Shenzhen Hospital, Shenzhen Peking University-Hong Kong University of Science and Technology Medical Center, Shenzhen 518036, China, e-mail: chenyun6308@139.com
ORCID: Mengxin Wang 0000-0001-9282-4493; Tingting Zheng 0000-0003-0424-0231

studies, we focused on damage assessment at cellular and molecular levels.

Keywords: focused ultrasound, blood, brain barrier, oxidative stress injury, reactive oxygen species

1 Introduction

Brain homeostasis is maintained by the blood–brain barrier (BBB), which is a barrier to the treatment of neurological diseases and restricts the entry of substances into the central nervous system (CNS). The tight junctions between capillary endothelial cells limit the diffusion of pathogenic microscopic organisms and prevent hydrophilic molecules larger than ~400 Da from the bloodstream into the brain parenchyma [1]. The BBB is the primary obstacle to the efficient intracerebral delivery of pharmaceuticals developed to treat neurological diseases [2,3]. Of the various existing techniques to deliver therapeutics to the brain, osmotic or chemical disruption of the BBB or direct neurosurgical injection are limited by high invasiveness, poor spatial distribution or low efficacy [4–6]. Therefore, modulation of the BBB has become a vital target for the treatment of CNS diseases [7,8].

Twenty years ago, it was demonstrated that focused ultrasound (FUS) combined with microbubbles (MBs) could be used to disrupt the BBB in a noninvasive and transient manner [9]. The BBB opening, using FUS in conjunction with MBs, is an attractive method for noninvasive penetration of the BBB due to its transient effect on the vasculature. The use of FUS has gained attention for its potential application in neurological disorders. In addition to the ablative [10,11] and sonodynamic therapy uses of FUS [12], current research is focused on the use of the FUS-induced BBB opening for drug delivery in preclinical therapeutic studies and clinical trials [13,14]. Safety studies were performed to investigate potential short-term histological evidence of post-treatment damage and adverse effects on behavioral readouts [15]. Functional magnetic resonance imaging (fMRI), a noninvasive tool, is one of the commonly used modalities [16]. Recent Phase I and Phase II clinical trials have shown the technology to be safe, reversible and reproducible in humans [17–20].

As preclinical evidence accumulated indicating that the approach was both effective and safe, researchers have deployed FUS-BBB openings for drug delivery to treat a wide range of brain disorders [3,21]. This method enhances the delivery of drugs to the CNS [15,22]. This safety has also been demonstrated in small animals and in non-human primates through histological evaluation and behavioral studies following FUS-BBB disruption [22,23]. The approach is usually combined with magnetic resonance imaging (MRI), which enables the treatment guidance, the evaluation of BBB disruption using MR contrast agents and the monitoring of potential damages during the procedure [9,24]. As with any new medical technique, most studies on FUS-BBB opening have focused on optimizing procedures to improve efficacy and demonstrate safety. In this work, we focused on parameters that effectively open the BBB and avoid oxidative damage to tissues, providing a basis for future experiments.

2 Results and discussion

2.1 Parameters screening of FUS

To determine BBB opening efficiency and damage caused by sonication, Evans Blue (EB) extravasation was confirmed according to the parameters shown in Table 1. We found that when the transducer frequency was 0.7 mHz ($n = 6$), almost no EB exosmosis was observed, indicating no BBB opening. However, when the frequency of the transducer is 0.9 mHz ($n = 6$), slight damage to brain tissue and skin burn on the brain surface can be observed, indicating that the frequency parameter is too high. Therefore, the frequency parameter is finally selected as 0.8 mHz. Peak pressure parameters were screened from 600 to 1,000 with a gradient of 100, and 900 mVpp was finally selected. The parameters of irradiation time are 30, 60 and

Table 1: Orthogonal experimental design

Case	Frequency (mHz)	Ppeak (mVpp)	Time (s)
1	0.9	700	90
2	0.9	800	60
3	0.9	900	30
4	0.8	700	60
5	0.8	800	90
6	0.8	900	90
7	0.8	1,000	30
8	0.7	700	30
9	0.7	800	90
10	0.7	900	60
11	0.6	800	30
12	0.6	1,000	90
13	0.6	700	60
14	0.9	1,000	60
15	0.7	1,000	90
16	0.6	900	90

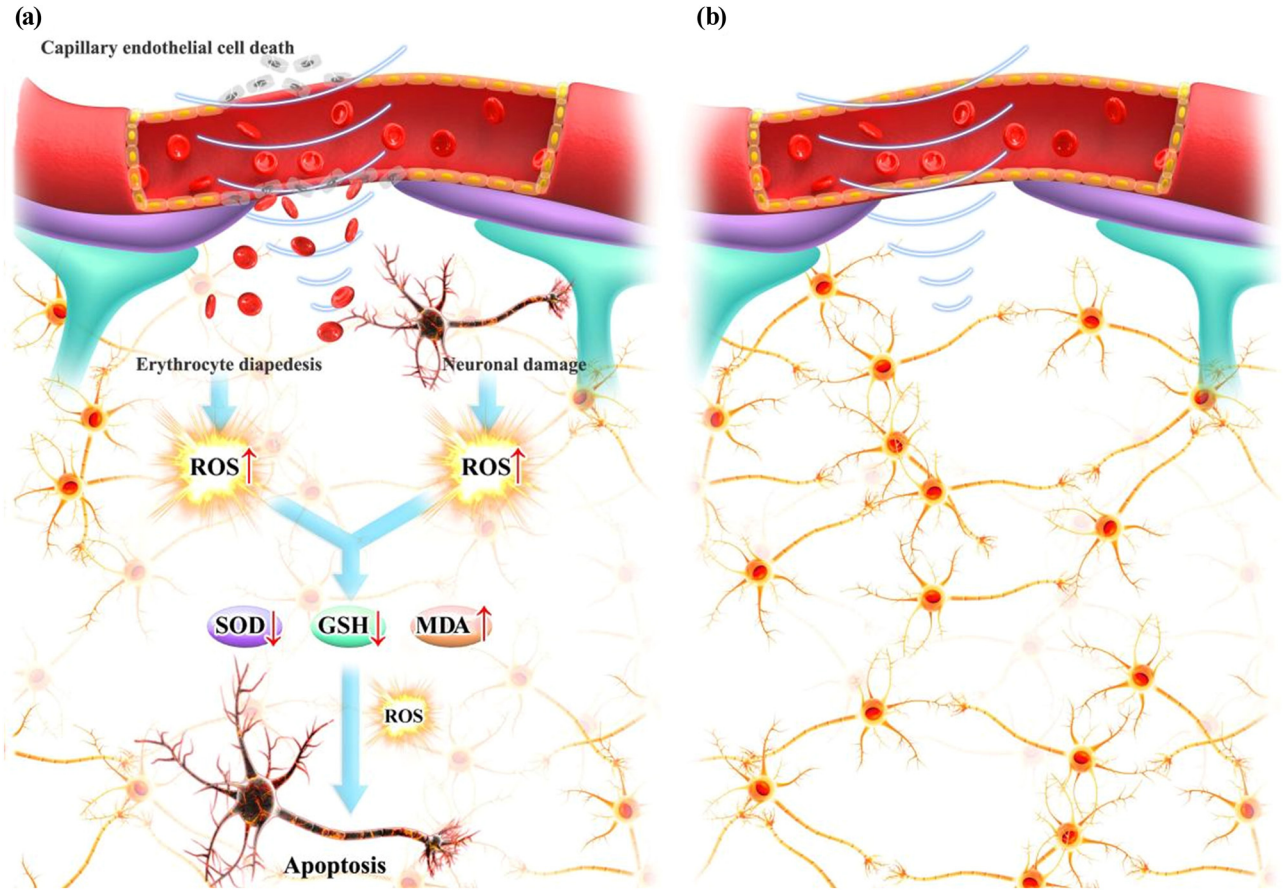

Scheme 1: Comparison of the effects of FUS open BBB injury and non-injury parameters. (a) The BBB opening accompanied by oxidative damage of capillary endothelial cells and neurons under the action of injury parameters, which induces the generation of reactive oxygen species (ROS), decreases of serum inflammatory factors glutathione (GSH) and superoxide dismutase (SOD), increases of malondialdehyde (MDA) and induces neuronal apoptosis. (b) BBB opening under the non-damaging FUS parameter.

90 s. The influence of irradiation time on the degree of BBB openness is positively correlated but has nothing to do with damage. Scheme 1 compares the effects of BBB injury and non-injury opening parameters. Under the action of injury parameters, oxidative damage leads to the apoptosis of vascular endothelial cells and neuron cells. Figure 1 shows representative results for evaluating the effectiveness of FUS-BBB opening by EB exudation, and other results are presented in the supporting information.

To summarize, when the frequency of the transducer is 0.8 mHz, the Ppeak is 800 mVPP and the irradiation time is 90 s; when the Ppeak is 900 mVPP and the irradiation time is 60 s, the BBB opening rate is 83% (n = 6); and when the Ppeak is 900 mVPP and the irradiation time is 90 s, the BBB opening rate is 100% (n = 6). The Ppeak of 1,000 mVPP and the irradiation time of 60 s or 90 s can also produce a 100% BBB opening (n = 6). The statistical results are shown in Table 2.

2.2 Safety assessment of the FUS-BBB opening

2.2.1 Histologic evaluations [hematoxylin–eosin (HE)]

Figure 2a1–5 shows representative HE staining results from five different FUS treatment parameters. As shown in the figure, except for the condition of 1,000 mVpp + 90 s, there was no obvious hemorrhage of brain tissues, suggesting that other effective parameters would not cause obvious brain tissue damage, which is consistent with the general tissue figure shown in Figure 1.

2.2.2 Evaluation of ROS effects

Serological tests were performed in modest condition (0.8 mHz + 900 mVpp + 90 s) and high condition (0.8 mHz +

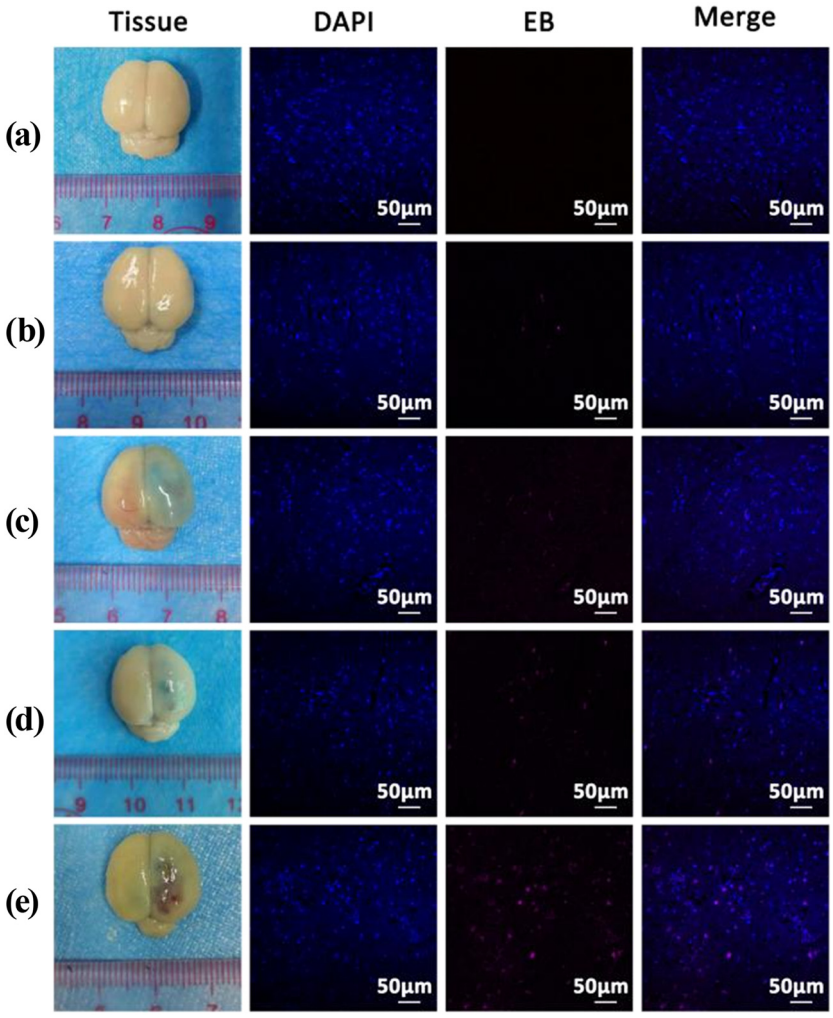

Figure 1: Brain tissue EB exudation under different parameters. (a) 0.8 mHz + 800 mVpp + 90 s, (b) 0.8 mHz + 900 mVpp + 60 s, (c) 0.8 mHz + 900 mVpp + 90 s, (d) 0.8 mHz + 1,000 mVpp + 60 s and (e) 0.8 mHz + 1,000 mVpp + 90 s. The pink fluorescence of the EB channel indicates that the BBB is successfully opened. Scale bar is 50 μm.

Table 2: Summary of optimum parameters

Frequency (mHz)	Ppeak (mVpp)	Irradiation time (s)	BBB open %	Safe (yes or no)
0.8	700	90	0	Yes
0.8	800	90	83	Yes
0.8	900	60	83	Yes
0.8	**900**	**90**	**100**	**Yes**
0.8	1,000	60	100	No
0.8	1,000	90	100	No

The line in bold shows the appropriate parameters obtained from the experimental data.

1,000 mVpp + 60 s) groups with 100% open BBB and no injury.

The GSH test results showed that compared with the control group, the GSH content in the suitable condition group was not significantly different, while the GSH content in the high condition group was significantly decreased (Figure 2b). The SOD detection results showed that compared with the control group, there was no significant difference in the SOD content in the suitable condition group, while the SOD content in the high condition group decreased significantly (Figure 2c). The MDA detection results showed that compared with the control group, there was no significant difference in the MDA content in the suitable condition group, while the MDA content in the high condition group increased significantly (Figure 2d). Thus, 0.8 mHz + 900 mVpp + 90 s is a more suitable parameter than 0.8 mHz + 1,000 mVpp + 60 s for BBB opening.

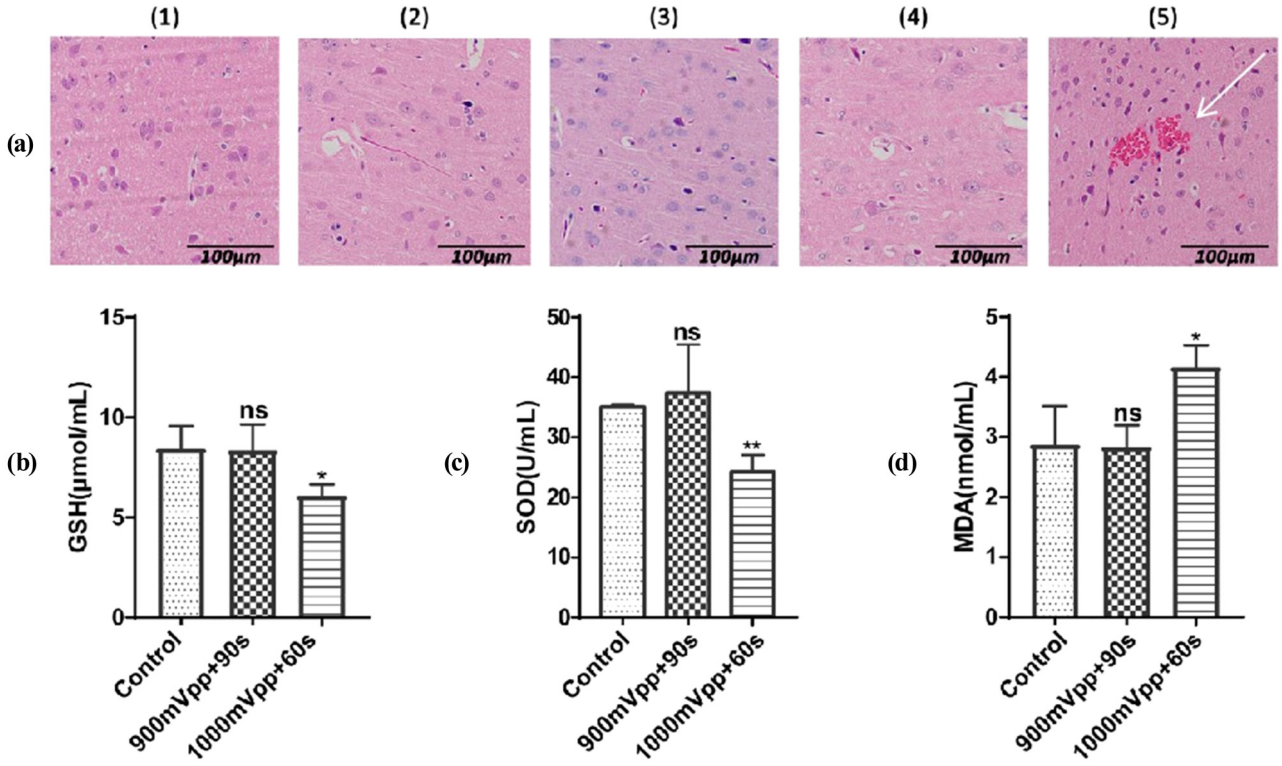

Figure 2: Safety of FUS-BBB opening. (a) HE staining of brain tissue under different parameters (400×): (a1) 800 mVpp + 90 s, (a2) 900 mVpp + 60 s, (a3) 900 mVpp + 90 s, (a4) 1000 mVpp + 60 s and (a5) 1000 mVpp + 90 s. White arrows represent obvious red blood cell exudation and bleeding. Legend is 100 μm. (b–d) Serological index results after 24 h of BBB opening.

2.2.3 Detection of apoptosis

TUNEL apoptosis staining was applied to rat brain tissue with different parameters; red fluorescence was observed in the two groups of 1,000 mVpp + 60 s (Figure 3d) and 1,000 mVpp + 90 s (Figure 3e). This indicates that the tissue cells underwent apoptosis, the fluorescence range was wider and the damage was more severe in the high condition group than in the low condition group. No obvious apoptosis was observed in the other condition groups (Figure 3a–c). Therefore, the transducer frequency of 0.8 mHz, Ppeak of 900 mVpp and irradiation time of 90 s were considered the best parameters for the effective and safe opening of rat BBB.

2.3 Supervision of BBB closure

Rats were imaged with T1-weighted MRI prior to FUS treatment, as shown in Figure 4a1 and b1. Immediately after FUS treatment, gadolinium (Gd) was injected into the tail vein, and the enhanced MRI (Figure 4a2 and b2) clearly showed typical Gd enhancement in rat brain tissue on T1-weighted imaging (indicated by black arrows), indicating that the BBB was successfully opened. At 24 h (Figure 4a3 and b3), the presence of the contrast agent in the FUS-irradiated site could still be observed, and it subsided compared with 0 h. The enhancement disappeared after 48 h (Figure 4a4 and b4). To further confirm our observations, EB was given intravenously after the FUS to demonstrate the extent of BBB opening in histology.

The successful opening of the BBB was confirmed by the exudation of EB dye at the sonication focal area. As shown in the tissue in Figure 5, the EB staining of gross histological specimens indicated the focal effect of ultrasound.

Microscopically, the opening of the BBB was further confirmed by using a confocal laser scanning microscope to detect EB in the brain parenchyma. To explore the exact time (under the optimal parameters) of the BBB closure in rats, a time gradient was set and EB was injected into the tail vein of FUS-treated rats at each time node. We obtained images of 6, 12, 24, 48, 72 and 96 h ($n = 6$). The BBB closings of rats at different times are summarized in Table 3. The general tissue image and confocal microscope results (Figure 5) show that local EB extravasation could be observed at 6, 12, 24, 48 and 72 h after sonication (EB observed in any individual in the same group was determined to be BBB unclosed); 12 h after sonication, we observed the maximum amount of

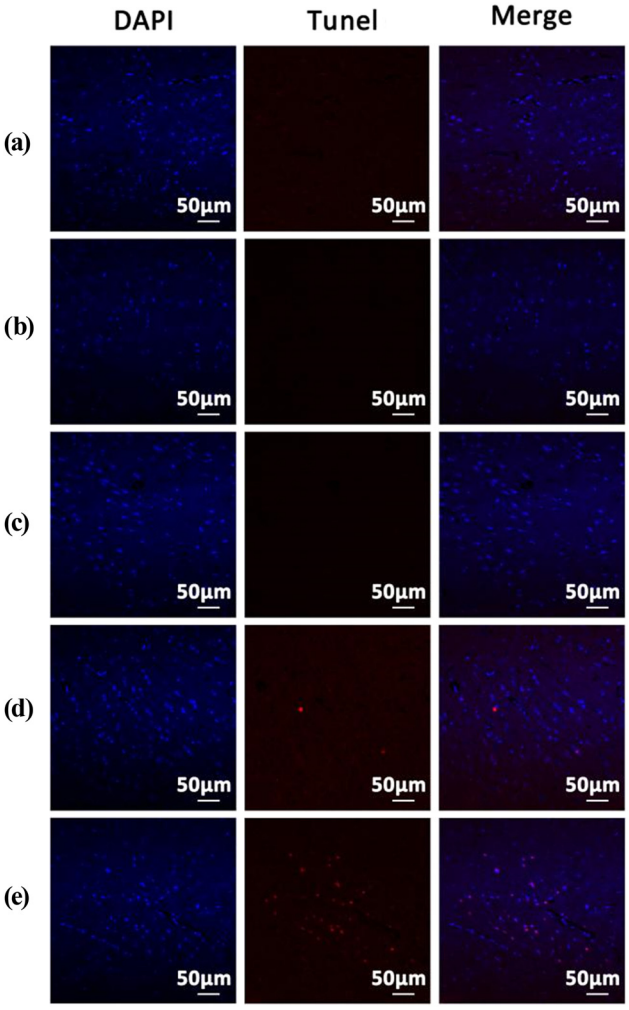

Figure 3: Safety of FUS-BBB opening. TUNEL apoptosis staining in brain tissue under different parameters: (a) 0.8 mHz + 800 mVpp + 90 s, (b) 0.8 mHz + 900 mVpp + 60 s, (c) 0.8m Hz + 900 mVpp + 90 s, (d) 0.8 mHz + 1,000 mVpp + 60 s and (e) 0.8 mHz + 1,000 mVpp + 90 s. Red fluorescence indicates apoptosis of tissue cells. The scale bar is 50 μm.

EB extravasation; and 96 h after sonication, no signs of BBB opening were found. Therefore, we believe that the BBB closure time at the microlevel is 96 h, and the BBB opening degree in rats reaches its maximum at 12 h and then decreases gradually over time.

The purpose of this study was to select the optimal BBB opening parameters through an orthogonal design, observe neuronal cells at the histological level to evaluate the safety of FUS-BBB opening and focus on the dynamic changes of BBB opening after sonication. In terms of safety, previous studies have mostly assessed brain tissue damage or apoptosis by HE staining [26]. During the 21st century, with the development of fMRI, some studies have begun to use fMRI technology to evaluate the changes in resting-state functional magnetic resonance imaging (rs-fMRI) indicators to determine the safety of FUS-BBB opening [16]. The principle of fMRI imaging is to measure the signal based on blood oxygen level-dependent (BOLD) changes. However, it has also been shown that an FUS-BBB opening leads to a significant reduction in the magnitude and duration of BOLD responses in target regions in the context of stimulus-induced neuronal activity, and the authors suggest that FUS-BBB opening may lead to local changes in cerebral neurovascular physiology [27]. This suggests that even a safe level of FUS-BBB opening can have an effect on BOLD changes [16]. Therefore, in this study, the effects of BBB opening induced by FUS on serum inflammatory factors were observed. On the issue of BBB closing time, MRI enhancement results (Figure 4) are not completely consistent with microscopic results (Figure 5), possibly due to the insufficient resolution of MRI.

In recent years, many preclinical studies have explored BBB open parameters in animals due to FUS's potential to noninvasively open the BBB for targeted therapy of brain diseases. Unfortunately, there are big differences in the animals, equipment and parameter settings. In our study, we used male Sprague Dawley (SD) rats to create the perfect conditions for safe BBB opening by screening different parameters. It is still unclear whether there is a link to the weight of SD rats as a safe parameter. A 2018 study by Gerstenmayer et al. indicated that skull thickness in SD rats of different ages and body weights was linearly proportional to body weight and that FUS loss through the skull increased linearly with body weight and frequency [28], BBB closure time and FUS parameters and MB dose parameters in BBB opening by FUS. Furthermore, this study was conducted in a healthy SD rat and the translation to a disease model was not discussed. In CNS diseases, brain tissue is in a pathophysiological state, and its BBB is also different from that of healthy tissue [29]. Therefore, future research needs to add disease models to assess the effect of disease status on the FUS-BBB opening.

3 Experimental

3.1 Animals

Male SD rats (8 weeks old, weighing 180–200 g) were used in this study. The animals were housed in a room maintained at 20–25°C, with access to food and water ad libitum in a 12-h/12-h light–dark cycle. All animal procedures were approved by the Animal Care and Use Committee at Shenzhen PKU-HKUSTMedical Center (protocol number 2020-010) and are in accordance with the

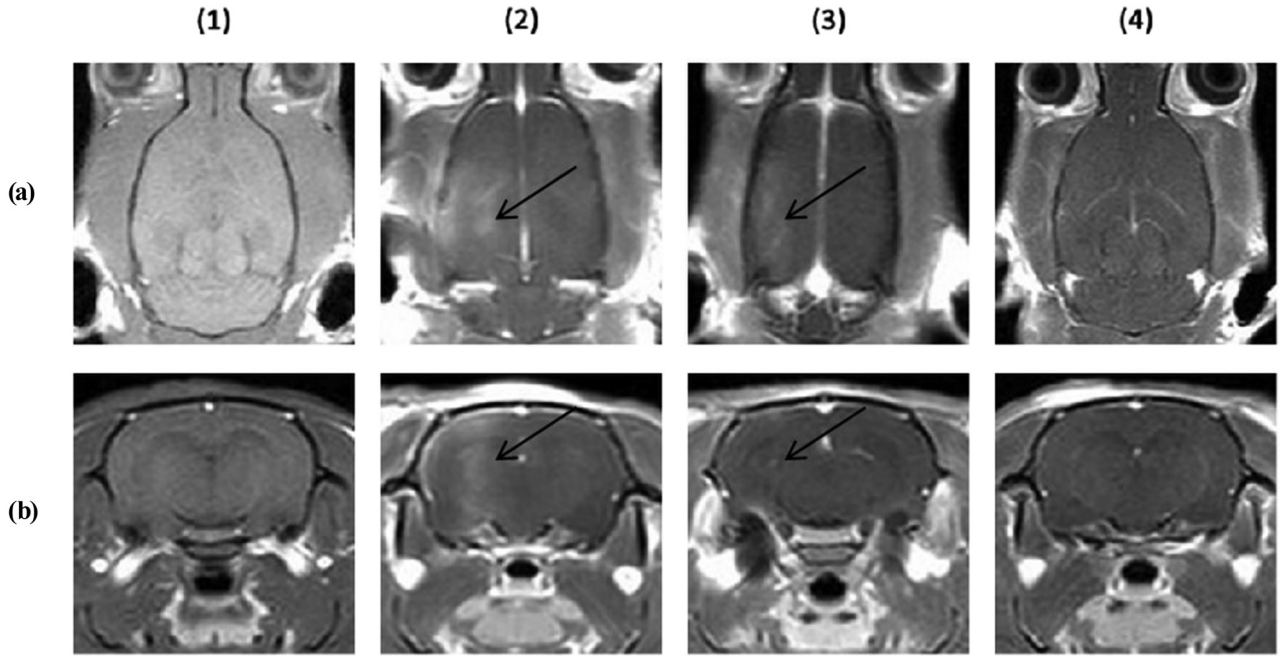

Figure 4: Enhanced MRI showing the opening and closure of the BBB. (a1 and b1) MRI T1-weighted scan before FUS opening the BBB. Images (a2–4) and (b2–4) are the T1 sequence scanning of MRI after ultrasound irradiation under appropriate parameters (0.8 MHZ + 900 mVpp + 90 s), and gadolinium contrast agent injection. Images (a1–4) are coronal positions, and images (b1–4) are horizontal positions. Images (a2) and (b2) are 0 h after BBB opening; images (a3) and (b3) are 24 h after BBB opening; and images (a4) and (b4) are 48 h after BBB opening. The black arrow indicates the area of enhancement.

guidelines of the Animal Experiments of the National Institutes of Health.

3.2 Animal preparation

All animals were acclimatized for 7 days before the study. At the beginning of the experiment, anesthetic induction was achieved via intraperitoneal (IP) injection of 1% pentobarbital sodium. Then, the heads of all animals were shaved with clippers and the hair over the skull was removed with depilatory cream. During the experiments, a heating pad was used to maintain body temperature and a tail vein catheter was used for injections of MBs, EB or MRI contrast agent.

3.3 FUS-induced BBB opening

The FUS instruments used in this study comprised a function generator, a radio frequency power amplifier and an FUS transducer with a diameter of 50 mm. The transducer was submerged in a water tank filled with deionized or degassed water and calibrated using a hydrophone [25]. The animals were placed in the prone position with their heads fixed by ear bars and coupled to the ultrasound transducer using ultrasound gel. This procedure was performed by applying FUS sonication immediately after intravenous (IV) injection of Sonovue MBs (5 mL/kg). The sonication parameters were designed as shown in Table 1.

3.4 EB staining

A 2% EB dye (2 mL/kg) was administered via the caudal vein after sonication to assess the influence of FUS with MBs on BBB opening. The animals were sacrificed 24 h after injection and perfused with saline solution to remove blood, and then, brain tissue was removed and collected for the following evaluations. The permeability of the BBB was evaluated by the exudation of EB in the brain tissue.

3.5 Histological evaluation

To assess brain tissue damage due to BBB opening by ultrasound stimulation, HE and TUNEL staining were performed (n = 3). Immediately after ultrasound exposure, EB dye was IV-injected to be an indicator of BBB opening. All animals were anesthetized with IP-injected 1% pentobarbital sodium, sacrificed 24 h after sonication, and perfused with saline solution to remove blood. For

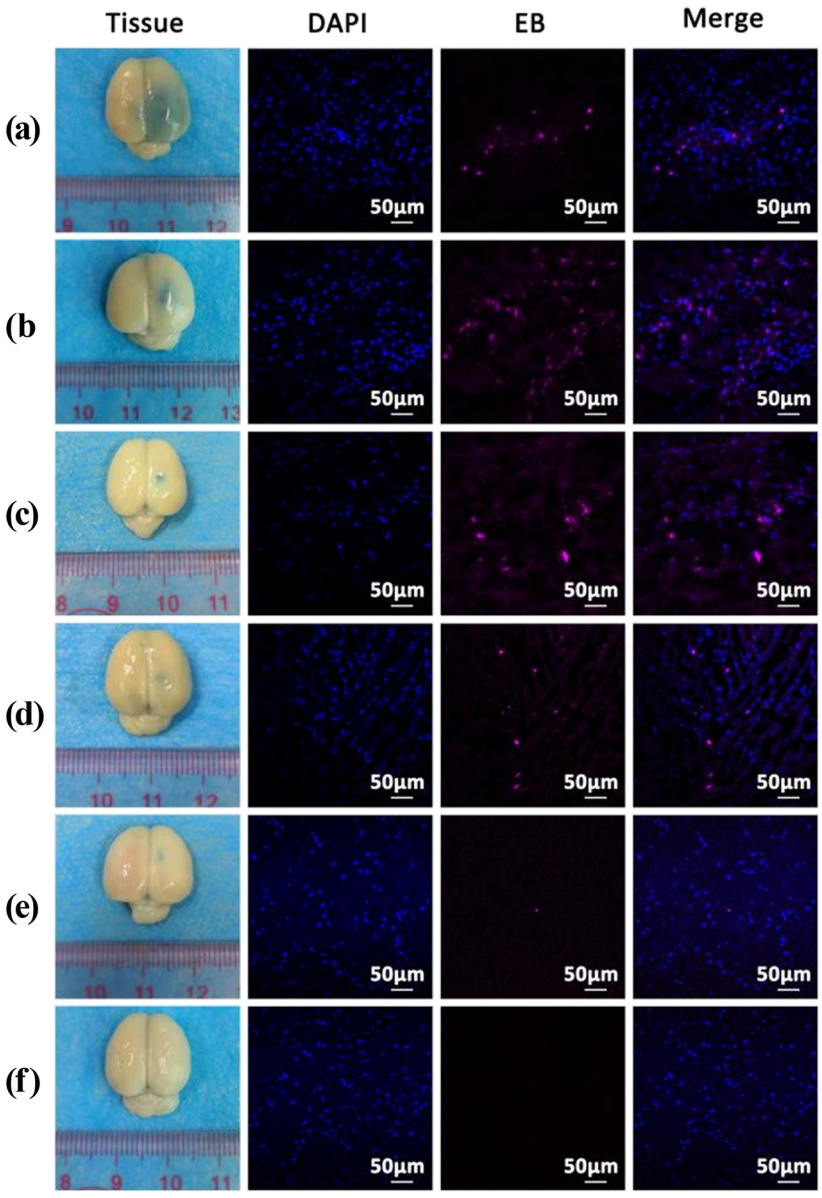

Figure 5: Duration of BBB opening. Representative brain tissue gross blue staining and EB confocal images at different time points after FUS opening the BBB: (a) 6 h, (b) 12 h, (c) 24 h, (d) 48 h, (e) 72 h and (f) 96 h. Pink fluorescence indicates that the tissue EB deposition. Scale bar is 50 μm.

Table 3: Summary of BBB closure

Groups	Time (h)	BBB closure (%)
1	0	0
2	6	0
3	12	17
4	24	50
5	48	50
6	72	77
7	96	100

HE staining, the harvested animal brains were fixed in 10% buffered neutral formalin, and the blue-stained focal region was dehydrated and embedded in paraffin. The brains were axially cut, using a vibratome of 5 μm thickness and stained with HE. Microscopic sections were performed at 200 magnification to evaluate histological images. For TUNEL staining, the EB extravasation area of brain sections was cut at 5 μm in thickness, using a cryotome and the staining was performed with a cell death detection kit. A fluorescence microscope was used to evaluate images.

3.6 Evaluation of ROS serum indicator levels (GSH, SOD, MDA)

Blood was collected and centrifuged at 3,000 rpm for 10 min, and the supernatant was taken for detection according to the GSH, SOD and MDA detection kit (A006-1, A001-3 and A003-4-1, Nanjing Jiancheng) instructions.

3.7 Confocal microscopy

Confocal laser scanning microscopy (Zeiss LSM700) equipped with at least four laser lines (405, 488, 568 and 647 nm) was used to make sure that the EB entered the brain tissue. EB can be exited at 647 nm with red fluorescence. We used a sequential scan to detect the nuclei stained with 4′,6-diamidino-2-phenylindole using a 405 nm laser and a 647 nm laser for EB.

3.8 MRI

The MRI scanner adopted a standard 3.0T signal system (3.0T MRI; Philips, Ingenia). We used a rat special nuclear magnetic coil (Suzhou Zhongzhi). During imaging, the rats were anesthetized with 1% pentobarbital. The imaging sequence and orientation were as follows: transverse and coronal T2WI: TR/TE = 1,200/60 ms, layer thickness/layer spacing = 1.0/0 mm, FOV = 60 mm × 60 mm, matrix = 256 × 256 and NSA = 3. After the ultrasound treatment, T2-weighted fast spin echo images were obtained, and a Gd (Prohance) MR contrast agent (1 mL/kg) was intravenously injected to detect and assess the opening of the BBB.

3.9 Statistical analysis

Statistical analysis was performed using GraphPad Prism (version 8.3.0, La Jolla, CA, USA). All experiments were performed at least three times. The values in the results section are expressed as mean ± standard deviation and were analyzed by *t*-test or one-way analysis of variance with a subsequent Bartlett's test. A statistical significance of 0.05 was accepted.

4 Conclusion

We successfully demonstrated that, in healthy SD rats, by combining three different parameters, the optimal parameters for opening the BBB in rats were screened and the duration of BBB opening was explored. At the same time, our experimental study verified its efficacy and safety at the histological and cellular levels. Under optimal parameter conditions, FUS-BBB opening showed no structural abnormalities, edema or hemorrhage and decreased the ROS effect at the tissue level compared with other parameters. In conclusion, these findings provide new evidence for the safety of FUS to open the BBB, suggesting its clinically translatable potential in the future treatment of brain diseases.

Funding information: MW and TZ thank grant No. JCYJ20210324131402008, No. KCXFZ20200201101048774, No. JCYJ20200109140212277 2022A1515010986, and No. 81901767. SG and YC acknowledge financial support from grant No. 81871358 and No. 2022A1515010296 and No. JCYJ20210324110211031. AH thanks grant No. JCYJ20180507183224565 and No. JCYJ20180223181216494, and LL thanks financial support from grant No. ZDSYS201504301045406 and No. JCYJ20210324110015040. BL thanks financial support from grant No.82102119. All authors thank Shenzhen Key Medical Discipline Construction Fund No. SZXK051, Guangdong High-level hospital construction fund No. GD2019260 and Sanming Project of Medicine in Shenzhen No. SZSM202111011.

Author contributions: MW – experiment, writing – original draft, investigation; SG – experiment, writing – original draft, validation; BL – investigation and experiment; TL – experiment; ZZ – experiment; DH – experiment; AH – data analysis; BX – experiment and data analysis; YQ – resources; LL – writing – review & editing, supervision; GC – writing – review & editing, resources; YC – writing – review & editing, funding acquisition; and TZ – project manager, writing – review & editing, funding acquisition.

Conflict of interest: There are no conflict to declare.

Ethical approval: All animal procedures were approved by the Animal Care and Use Committee at Shenzhen PKU-HKUSTMedical Center (protocol number 2020-010) and are in accordance with the guidelines of the Animal Experiments of the National Institutes of Health.

Data availability statement: All data generated or analyzed during this study are included in this published article [and its supplementary information files].

References

[1] Abbott NJ, Patabendige AA, Dolman DE, Yusof SR, Begley DJ. Structure and function of the blood-brain barrier. Neurobiol Dis. 2010;37(1):13–25.

[2] Shin J, Kong C, Cho JS, Lee J, Koh CS, Yoon MS, et al. Focused ultrasound-mediated noninvasive blood-brain barrier modulation: preclinical examination of efficacy and safety in various sonication parameters. Neurosurg Focus. 2018;44(2):E15.

[3] Endo-Takahashi Y, Kurokawa R, Sato K, Takizawa N, Katagiri F, Hamano N, et al. Ternary complexes of pDNA, neuron-binding peptide, and PEGylated polyethyleneimine for brain delivery with nano-bubbles and ultrasound. Pharmaceutics. 2021;13(7):1003. doi: 10.3390/pharmaceutics13071003.

[4] Bajracharya R, Caruso AC, Vella LJ, Nisbet RM. Current and emerging strategies for enhancing antibody delivery to the brain. Pharmaceutics. 2021;13(12):2014. doi: 10.3390/pharmaceutics13122014.

[5] Hersh DS, Wadajkar AS, Roberts N, Perez JG, Connolly NP, Frenkel V, et al. Evolving drug delivery strategies to overcome the blood brain barrier. Curr Pharm Des. 2016;22(9):1177–93.

[6] Mo F, Pellerino A, Soffietti R, Rudà R. Blood-brain barrier in brain tumors: biology and clinical relevance. Int J Mol Sci. 2021;22(23):12654. doi: 10.3390/ijms222312654.

[7] Hawkins BT, Davis TP. The blood-brain barrier/neurovascular unit in health and disease. Pharmacol Rev. 2005;57(2):173–85.

[8] Han L. Modulation of the blood-brain barrier for drug delivery to brain. Pharmaceutics. 2021;13(12):2024. doi: 10.3390/pharmaceutics13122024.

[9] Hynynen K, McDannold N, Vykhodtseva N, Jolesz FA, Noninvasive MR. Imaging-guided focal opening of the blood-brain barrier in rabbits. Radiology. 2001;220(3):640–6.

[10] Paun L, Moiraghi A, Jannelli G, Nouri A, DiMeco F, Pallud J, et al. From focused ultrasound tumor ablation to brain blood barrier opening for high grade glioma: A systematic review. Cancers (Basel). 2021;13(22):13.

[11] Valdez MA, Fernandez E, Matsunaga T, Erickson RP, Trouard TP. Distribution and diffusion of macromolecule delivery to the brain via focused ultrasound using magnetic resonance and multispectral fluorescence imaging. Ultrasound Med Biol. 2020;46(1):122–36.

[12] Wu SK, Santos MA, Marcus SL, Hynynen K. MR-guided focused ultrasound facilitates sonodynamic therapy with 5-aminolevulinic acid in a rat glioma model. Sci Rep. 2019;9(1):10465.

[13] Meng Y, Hynynen K, Lipsman N. Applications of focused ultrasound in the brain: from thermoablation to drug delivery. Nat Rev Neurol. 2021;17(1):7–22.

[14] Schoen S, Jr., Kilinc MS, Lee H, Guo Y, Degertekin FL, Woodworth GF, et al. Towards controlled drug delivery in brain tumors with microbubble-enhanced focused ultrasound. Adv Drug Deliv Rev. 2022;180:114043.

[15] McDannold N, Arvanitis CD, Vykhodtseva N, Livingstone MS. Temporary disruption of the blood-brain barrier by use of ultrasound and microbubbles: safety and efficacy evaluation in rhesus macaques. Cancer Res. 2012;72(14):3652–63.

[16] Todd N, Zhang Y, Arcaro M, Becerra L, Borsook D, Livingstone M, et al. Focused ultrasound induced opening of the blood-brain barrier disrupts inter-hemispheric resting state functional connectivity in the rat brain. Neuroimage. 2018;178:414–22.

[17] Lipsman N, Meng Y, Bethune AJ, Huang Y, Lam B, Masellis M, et al. Blood-brain barrier opening in Alzheimer's disease using MR-guided focused ultrasound. Nat Commun. 2018;9(1):2336.

[18] Mainprize T, Lipsman N, Huang Y, Meng Y, Bethune A, Ironside S, et al. Blood-brain barrier opening in primary brain tumors with non-invasive MR-guided focused ultrasound: A clinical safety and feasibility study. Sci Rep. 2019;9(1):321.

[19] Gasca-Salas C, Fernández-Rodríguez B, Pineda-Pardo JA, Rodríguez-Rojas R, Obeso I, Hernández-Fernández F, et al. Blood-brain barrier opening with focused ultrasound in Parkinson's disease dementia. Nat Commun. 2021;12(1):779.

[20] Ngamcherdtrakul W, Bejan DS, Cruz-Muñoz W, Reda M, Zaidan HY, Siriwon N, et al. Targeted nanoparticle for co-delivery of HER2 siRNA and a taxane to mirror the standard treatment of HER2 + breast cancer: efficacy in breast tumor and brain metastasis. Small. 2022;18:e2107550.

[21] Timbie KF, Mead BP, Price RJ. Drug and gene delivery across the blood-brain barrier with focused ultrasound. J Control Rel. 2015;219:61–75.

[22] Liu X, Naomi SSM, Sharon WL, Russell EJ. The applications of focused ultrasound (FUS) in Alzheimer's disease treatment: A systematic review on both animal and human studies. Aging Dis. 2021;12(8):1977–2002.

[23] Pouliopoulos AN, Kwon N, Jensen G, Meaney A, Niimi Y, Burgess MT, et al. Safety evaluation of a clinical focused ultrasound system for neuronavigation guided blood-brain barrier opening in non-human primates. Sci Rep. 2021;11(1):15043.

[24] Ishida J, Alli S, Bondoc A, Golbourn B, Sabha N, Mikloska K, et al. MRI-guided focused ultrasound enhances drug delivery in experimental diffuse intrinsic pontine glioma. J Control Rel. 2021;330:1034–45.

[25] Grudzenski S, Heger S, de Jonge A, Schipp J, Dumont E, Larrat B, et al. Simulation, implementation and measurement of defined sound fields for blood-brain barrier opening in rats. Ultrasound Med Biol. 2021;48:422–36.

[26] Cho H, Lee HY, Han M, Choi JR, Ahn S, Lee T, et al. Localized down-regulation of P-glycoprotein by focused ultrasound and microbubbles induced blood-brain barrier disruption in rat brain. Sci Rep. 2016;6:31201.

[27] Rauscher A, Sedlacik J, Barth M, Haacke EM, Reichenbach JR. Nonnvasive assessment of vascular architecture and function during modulated blood oxygenation using susceptibility weighted magnetic resonance imaging. Magn Reson Med. 2005;54(1):87–95.

[28] Gerstenmayer M, Fellah B, Magnin R, Selingue E, Larrat B. Acoustic transmission factor through the rat skull as a function of body mass, frequency and position. Ultrasound Med Biol. 2018;44(11):2336–44.

[29] Tayler H, Miners JS, Güzel Ö, MacLachlan R, Love S. Mediators of cerebral hypoperfusion and blood-brain barrier leakiness in Alzheimer's disease, vascular dementia and mixed dementia. Brain Pathol. 2021;31(4):e12935.